nature sustainability

Article https://doi.org/10.1038/s41893-022-01056-7

Afforesting arid land with renewable electricity and desalination to mitigate climate change

In the format provided by the authors and unedited

Supplementary Information

Afforesting arid land with renewable electricity and desalination to mitigate climate change

Upeksha Caldera[1], Christian Breyer[1]
[1] LUT University, Yliopistonkatu 34, 53850 Lappeenranta, Finland

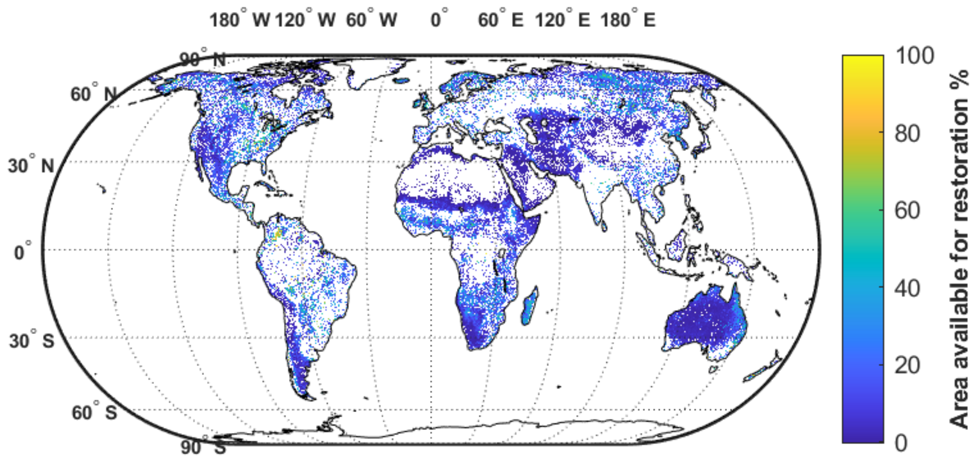

Figure S1. Tree cover available for restoration nodes (0.1° x 0.1° resolution). Minimum value of 0.0031% and maximum value of 100%. Original data extracted from Bastin et al. [1].

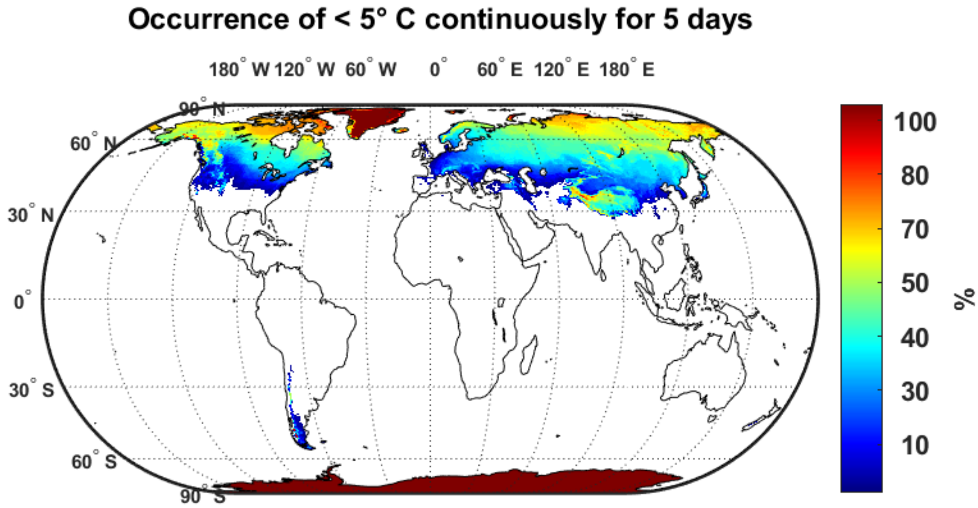

Figure S2. Coloured regions are those where average temperature is not more than 5°C for 5 days continuously. Global surface temperature data (for the year 2005) is taken from the NASA database[2]. Regions in white indicate those areas deemed suitable for the chosen tree mix since temperatures are higher than 5°C. Percentage indicates the number of times in the year, the temperature goes less than 5°C.

Table S1. Minimum extreme temperature range for the chosen trees obtained from the USDA Hardiness Zone map[3]. Climatic zone is obtained from the CUFR calculator[4]. Given the minimum extremes for all trees, the temp range that would be suitable for all trees was set to greater than 5°C.

		Climatic Zone on CUFR calcuator	**USDA Hardiness Zone**	**Minimum Extreme Temperature Range °C**
Tree 1	Eucalpytus Coolibah	SouthWest Desert	9 and 10	-6.7 to 4
Tree 2	Paperbark	Tropical	11	4.4 to 10
Tree 3	Date Palm	Tropical	11	4.4 to 11
Tree 4	Turkish Pine	Inland Empire	9	-6.7 to -1.1
Tree 5	Willow Acacia	SouthWest Desert	9 and 10	-6.7 to 4
Tree 6	Casuarina	Tropical	11	4.4 to 10
Tree 7	Kamani	Tropical	11	4.4 to 11
Tree 8	White Mulberry	SouthWest Desert	9 and 10	-6.7 to 4

Note S1. According to the FAO[5], for date palms, if very low temperatures are maintained for the time period between 12 hrs to 5 days, the leaves will show frost damage and the tree will appear burnt. This time period was considered and 5 days set as the time period for which the temperature should not drop less than 5°C.

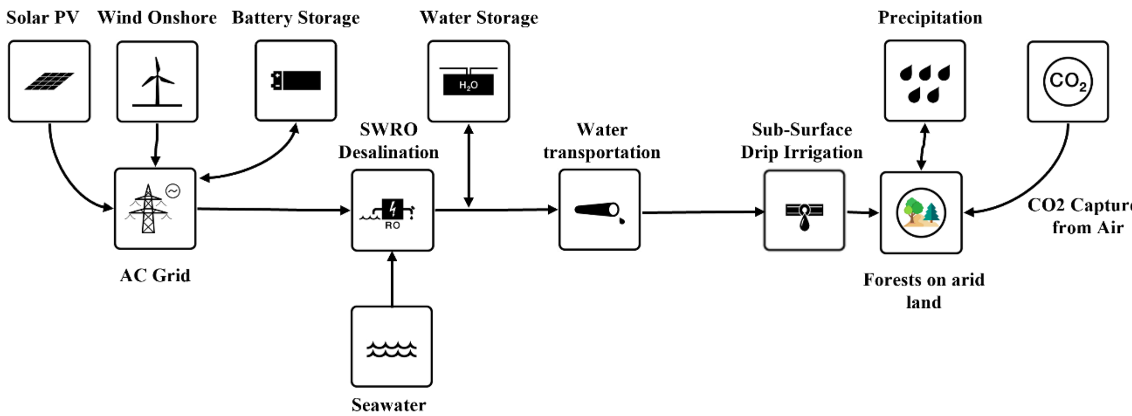

Figure S3. Outline of the concept presented in this research. Low-cost RE powered (mostly solar PV + wind + battery storage) SWRO desalinated water is pumped to areas on arid land with restoration potential or bare land with suitable conditions to grow forests. The forests are irrigated with sub-surface drip irrigation systems and as the canopy area of the trees increase, there is an increase in precipitation, capping out at 26% as explained in Figure S5. Th CO_2 is stored in the aboveground, belowground biomass as well as the soil, deadwood and litter of the forests.

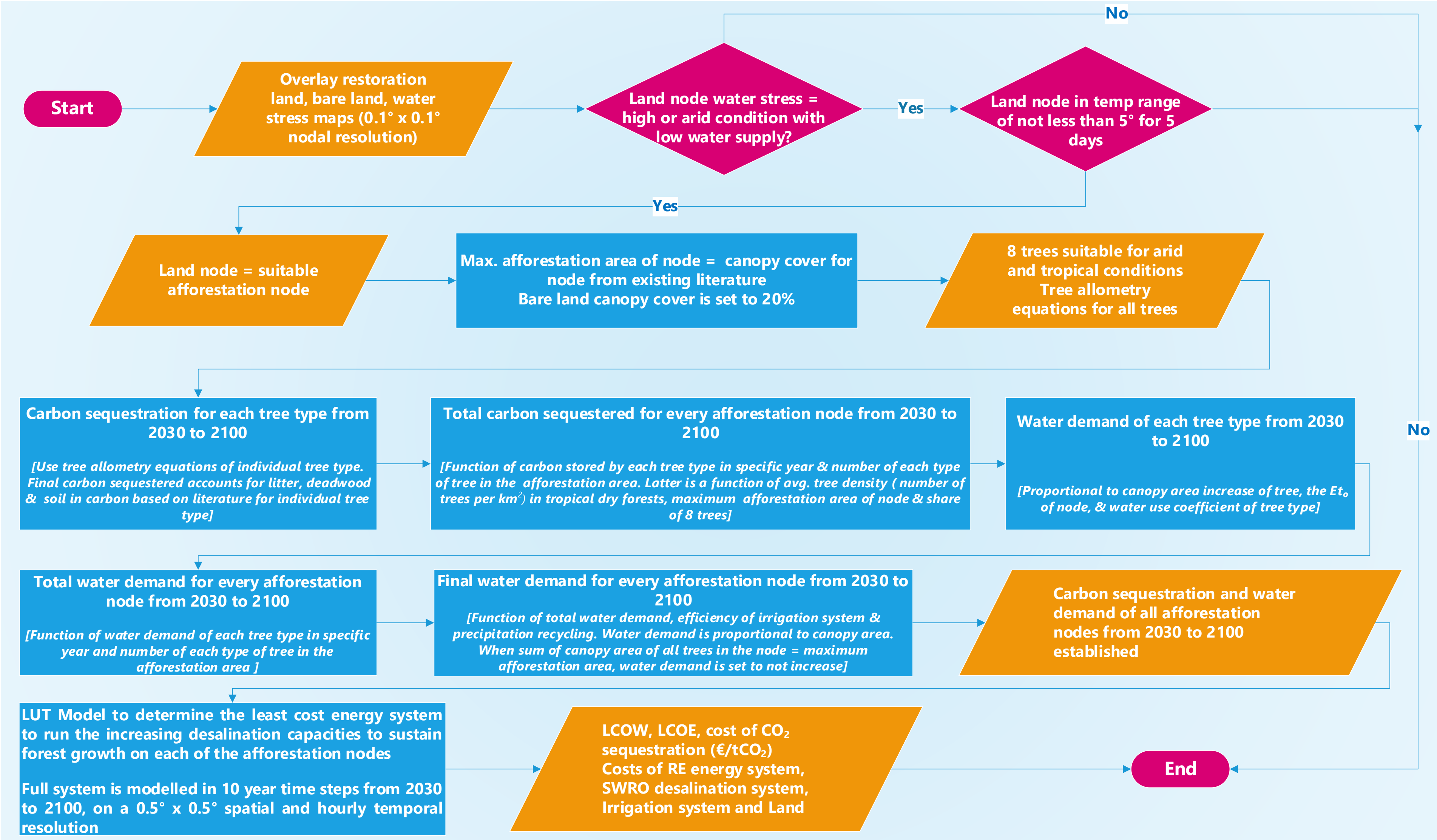

Figure S4. Flowchart presentation of the approach taken in this study.

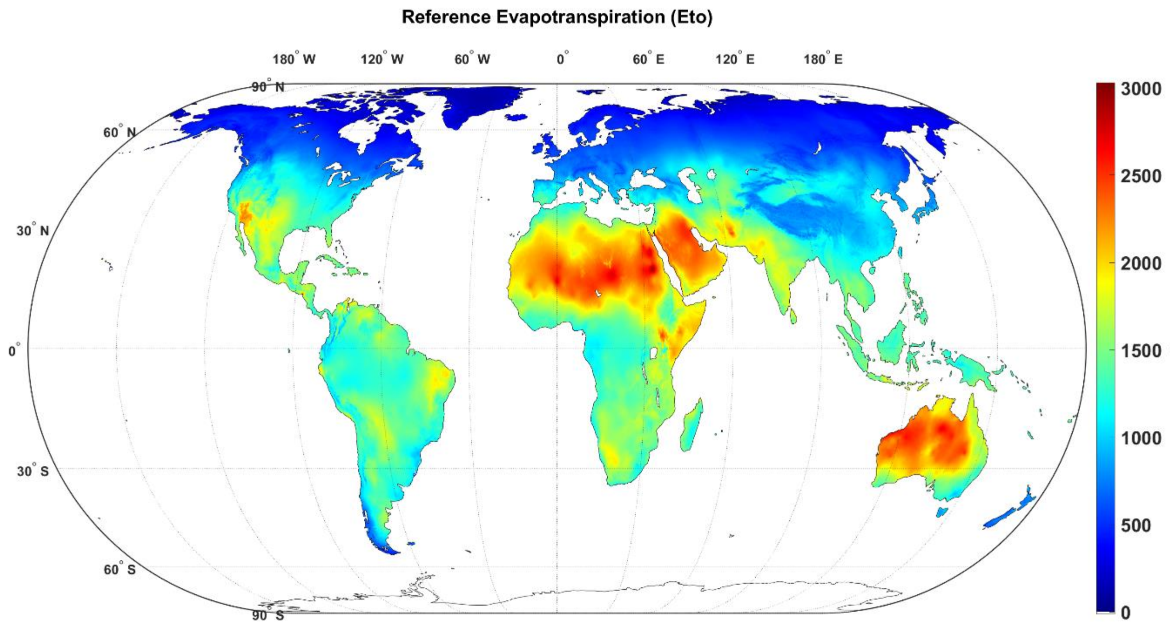

Figure S5. Global mean annual Reference Evapotranspiration values (0.1° x 0.1° resolution). Obtained from FAO Map Catalog[6]. These nodal values are used together with the tree species specific water use co-efficient to determine the water demand of the tree.

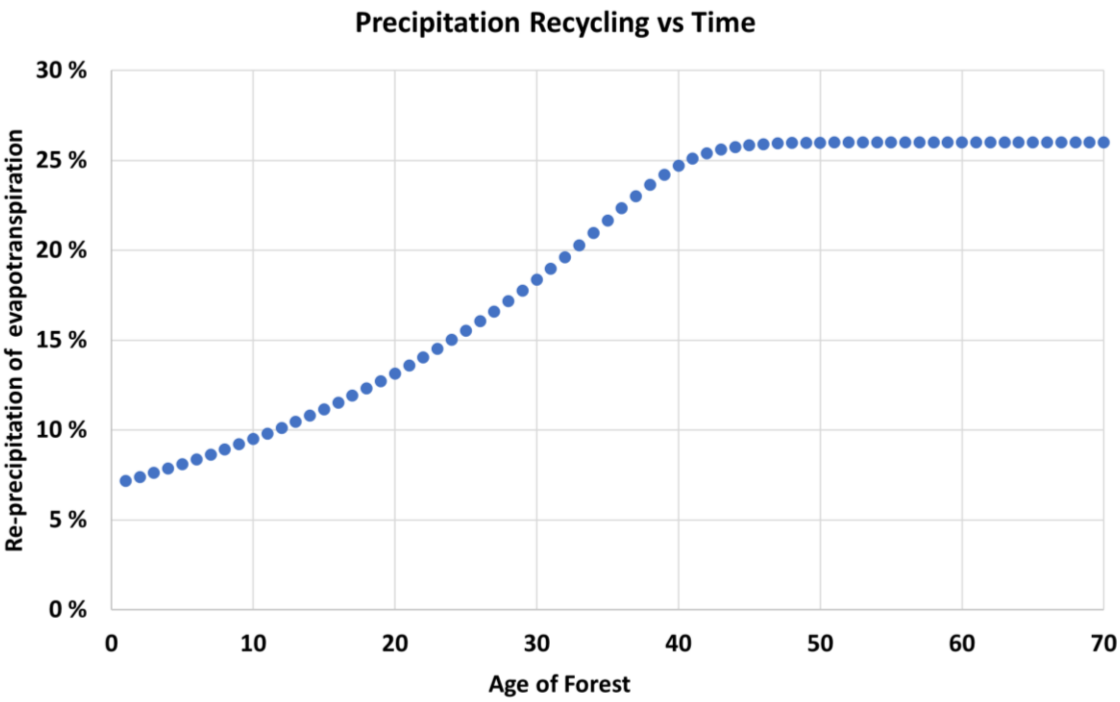

Figure S6. Share of evapotranspiration that may reprecipitate local over the afforested region. As the trees mature and canopy grows re-precipitation increases[7]. In the Sahara region, Kemena et al.[8] observed a 26% re-precipitation. This is set as the maximum value in this research to be reached when a forest matures in about 40 years.

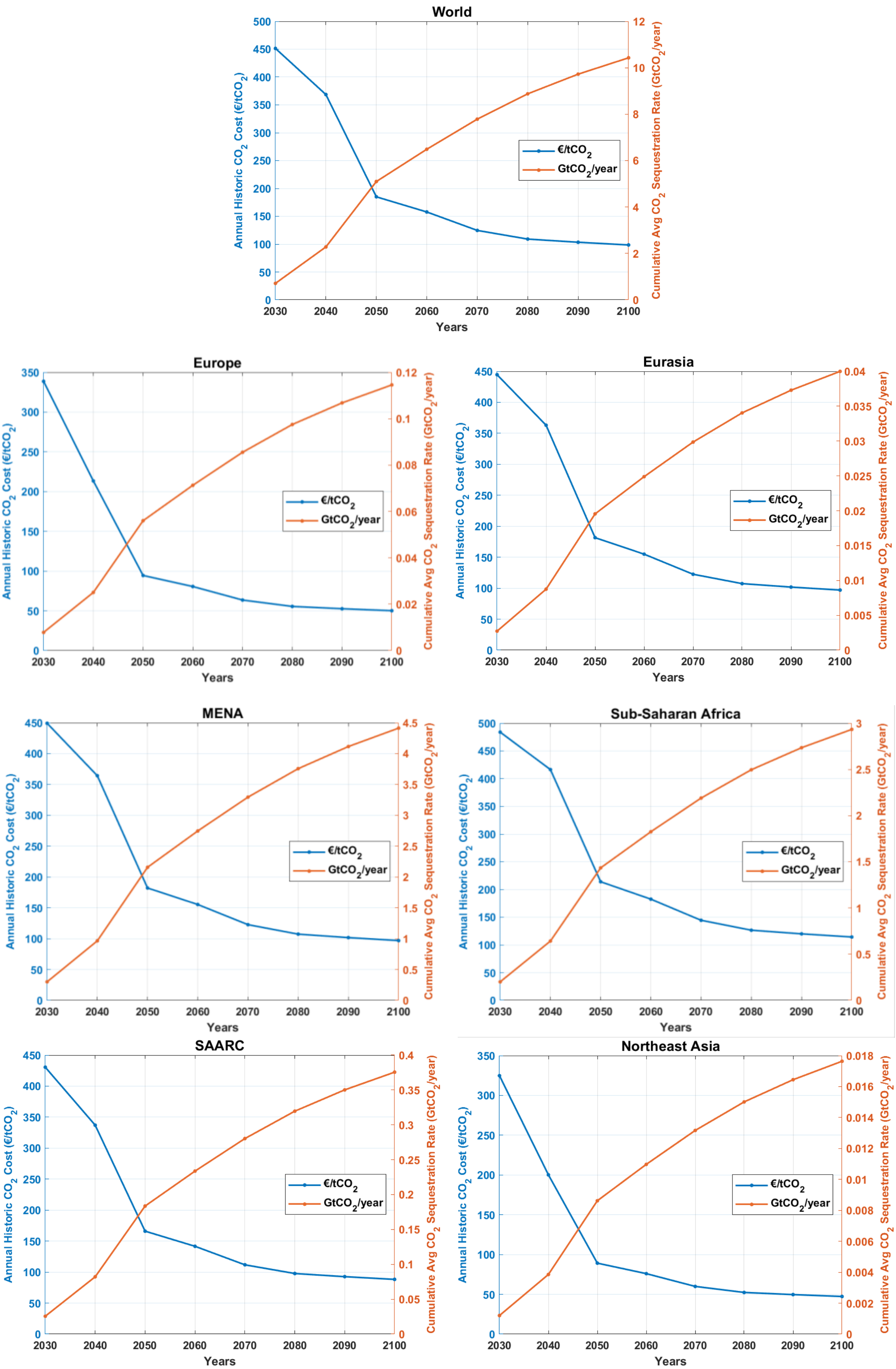
World
Europe
Eurasia
MENA
Sub-Saharan Africa
SAARC
Northeast Asia
Annual Historic CO2 Cost (€/tCO2)
Cumulative Avg CO2 Sequestration Rate (GtCO2/year)
Years
€/tCO2
GtCO2/year
2030
2040
2050
2060
2070
2080
2090
2100

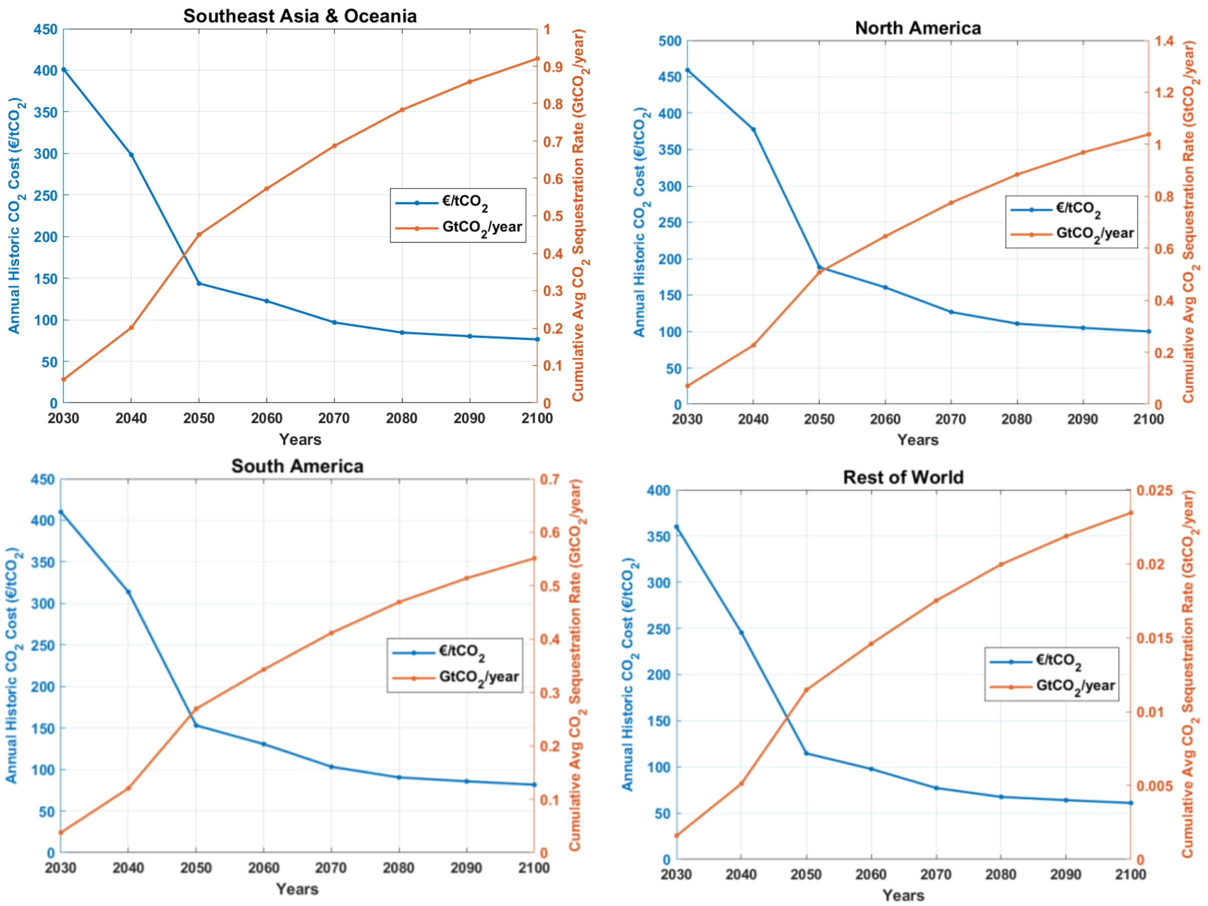

Figure S7. Annual historic CO_2 costs and CO_2 sequestration rate variation for the world and the major regions from 2030 to 2100. Climate zones that require more water have higher CO_2 costs since the cost is heavily driven by water demand.

The map diagram in the Figures S6 - S18 are in a 0.5° x 0.5° resolution.

(a)

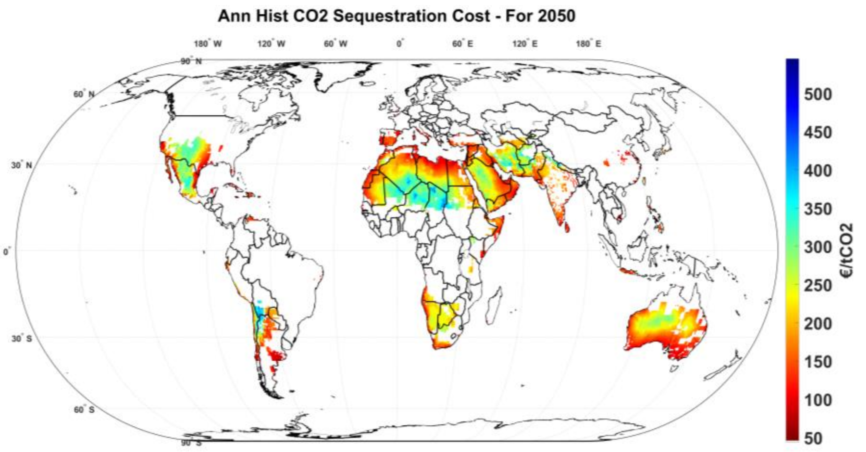

(b)

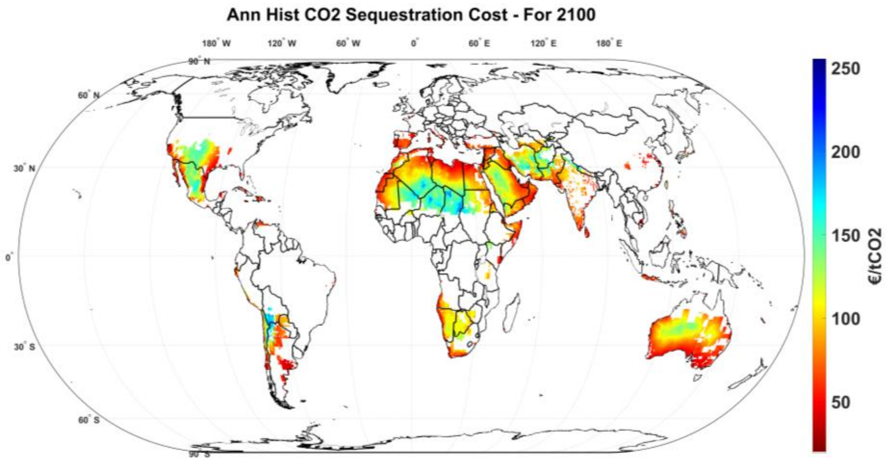

Figure S8. Annual historic CO_2 costs in a 0.5° x 0.5° resolution in 2050 (a); and 2100 (b).

(a)

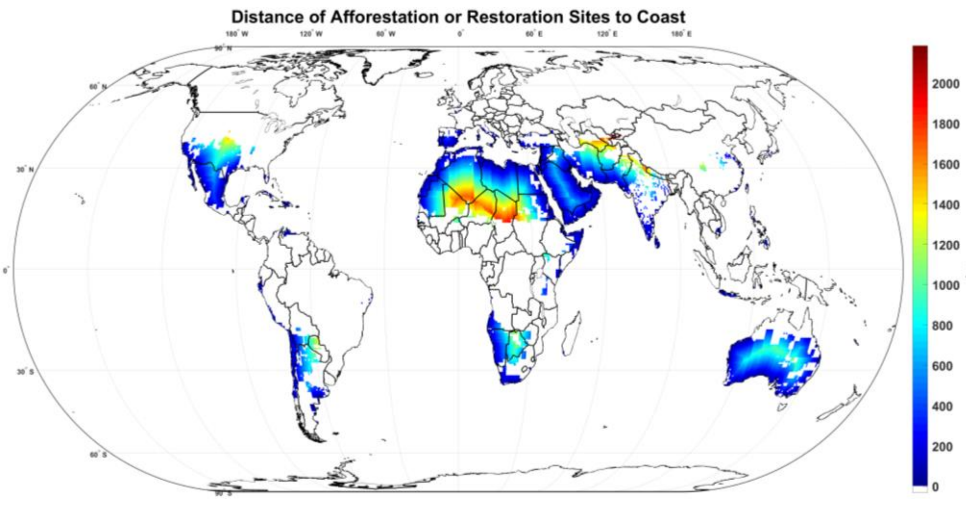

(b)

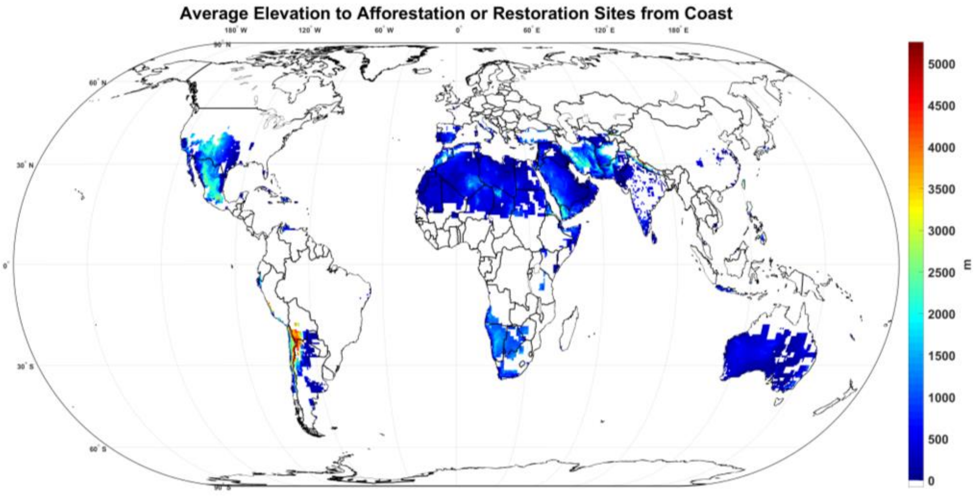

(c)

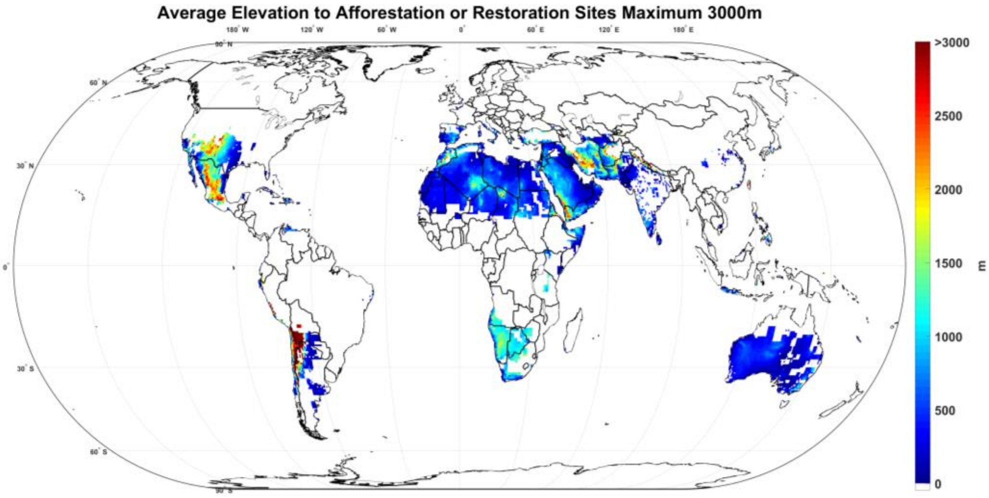

Figure S9. Average horizontal pumping distance to afforestation site from nearest coastline (a); Average elevation to afforestation sites (b); Average elevation with a maximum of 3000 m specified (c) Pumping energy accounts for both the horizontal and vertical transportation distances. The water transportation costs and energy consumption are sourced from literature as explained in Caldera and Breyer[9].

(a)

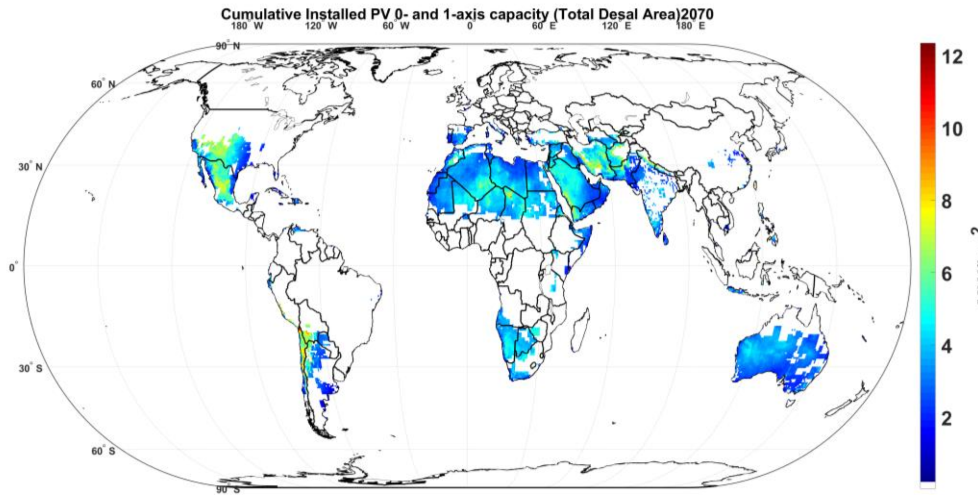

(b)

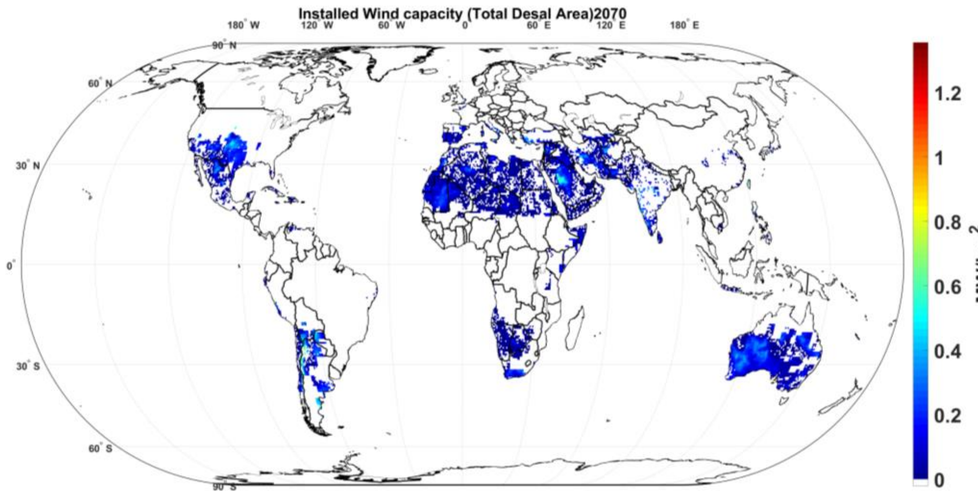

Figure S10. Cumulative solar PV single-axis tracking (PV 1) and fixed-tilted (PV 0) per unit of the total area that is afforested (a); Cumulative wind capacity per unit of the total area that is afforested. The excel results file Supplementary Information 3 provides the data on a country and yearly level, while the map diagrams show on a nodal level for the specific year 2070.

(a)

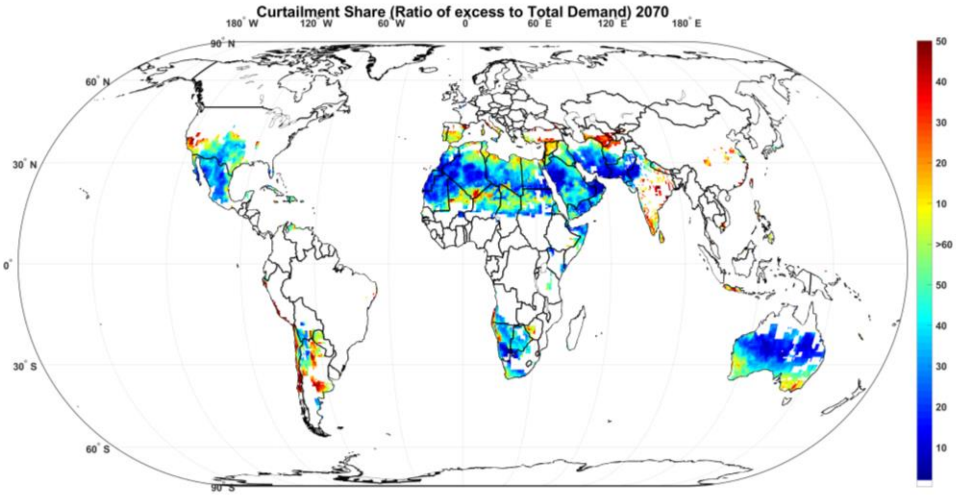

(b)

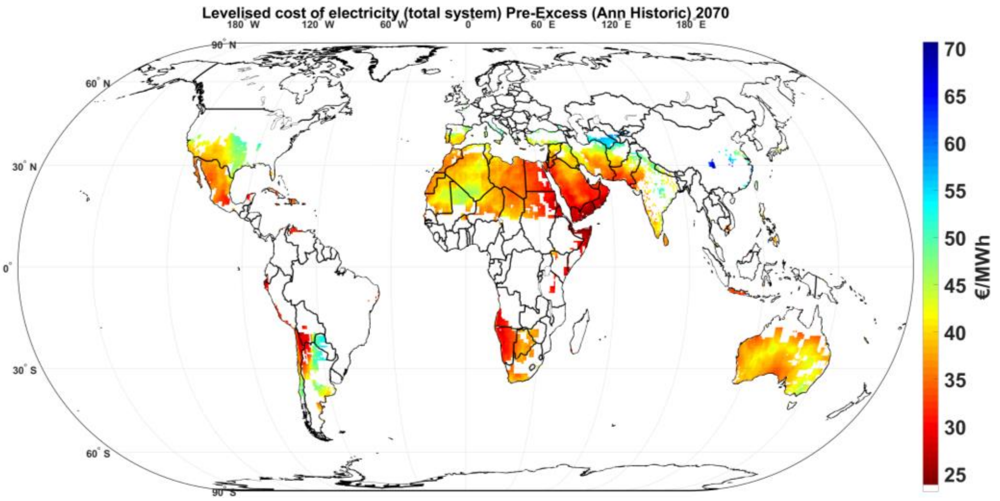

(c)

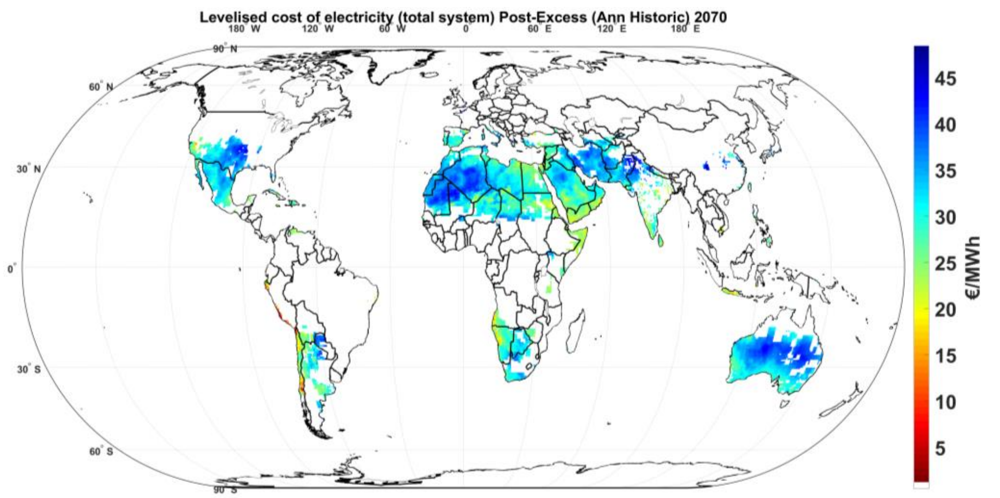

Figure S11. Ratio of the excess generation to the total demand. In an integrated energy system, this energy would be used by other sectors of the energy system. To emulate this effect, it was considered that the excess energy would be sold at the LCOE system value in (b). The excess would be brought down to 10%. The income gained from the excess sold is then used to calculate the new LCOE (c).

(a)

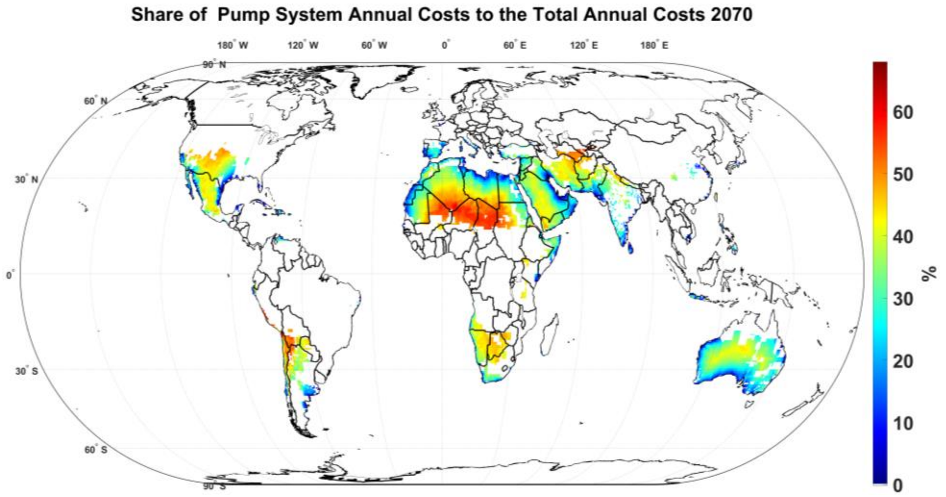
Share of Pump System Annual Costs to the Total Annual Costs 2070
180° W
120° W
60° W
0°
60° E
120° E
180° E
90° N
60° N
30° N
0°
30° S
60° S
90° S
60
50
40
30
20
10
0
%

(b)

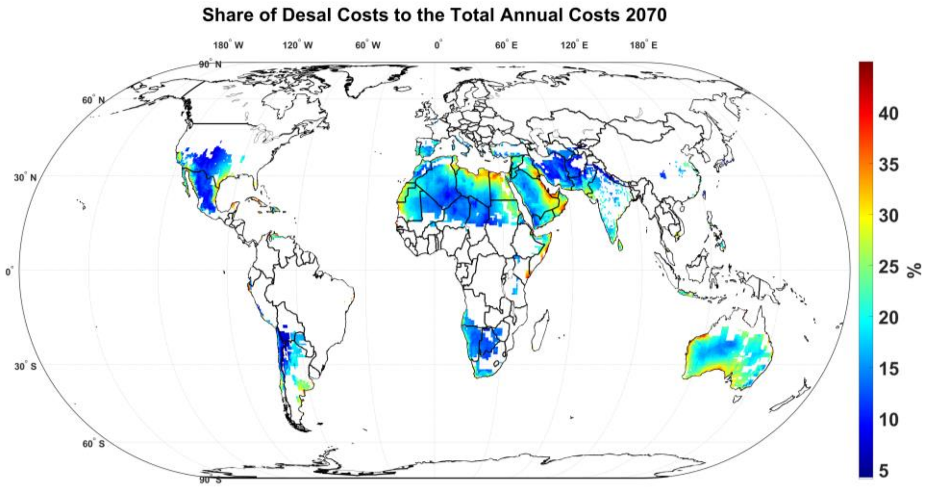
Share of Desal Costs to the Total Annual Costs 2070
180° W
120° W
60° W
0°
60° E
120° E
180° E
90° N
60° N
30° N
0°
30° S
60° S
90° S
40
35
30
25
20
15
10
5
%

(c)

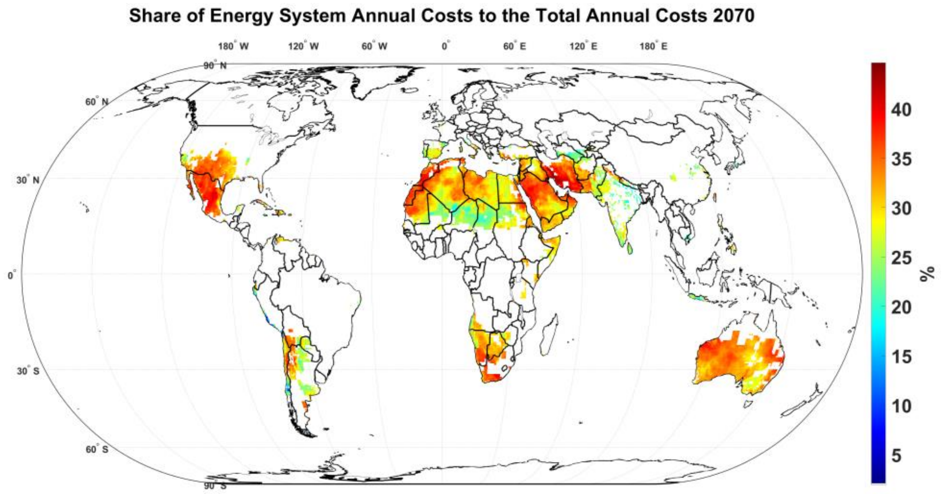
Share of Energy System Annual Costs to the Total Annual Costs 2070
180° W
120° W
60° W
0°
60° E
120° E
180° E
90° N
60° N
30° N
0°
30° S
60° S
90° S
40
35
30
25
20
15
10
5
%

(d)

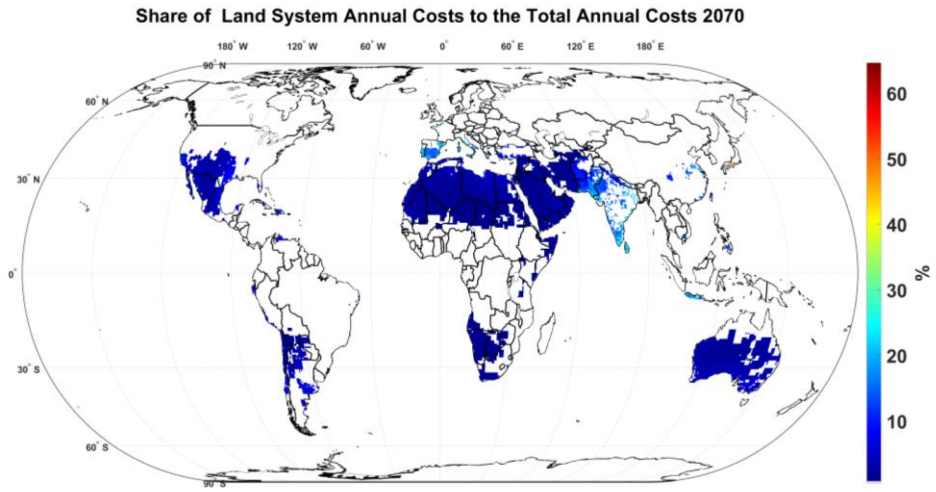

(e)

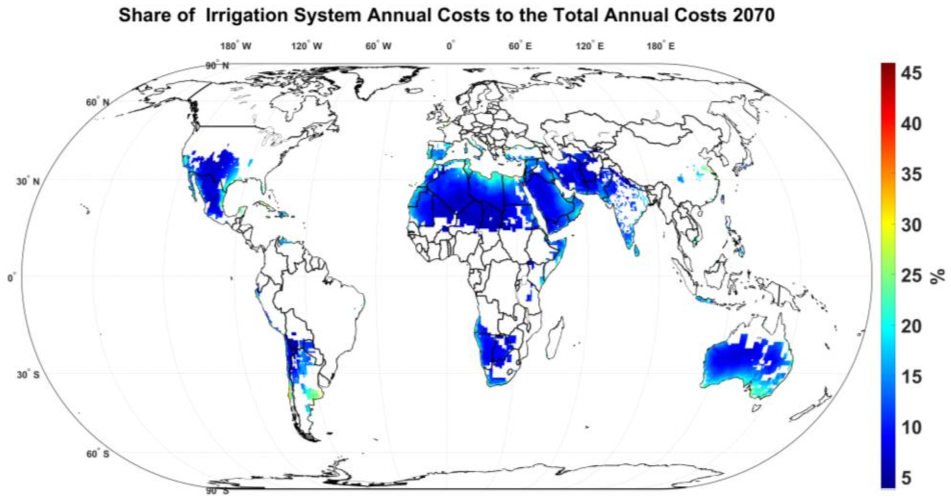

Figure S12. Contribution of the components that comprise the afforestation system presented in this research to the total annualised costs of the afforestation node: horizontal and vertical water pumping and piping infrastructure (a); SWRO desalination costs (b); RE-based energy system costs (c); Land costs dependent on region and further broken down in Figure 11 (d); sub-surface irrigation system costs (e).

(a)

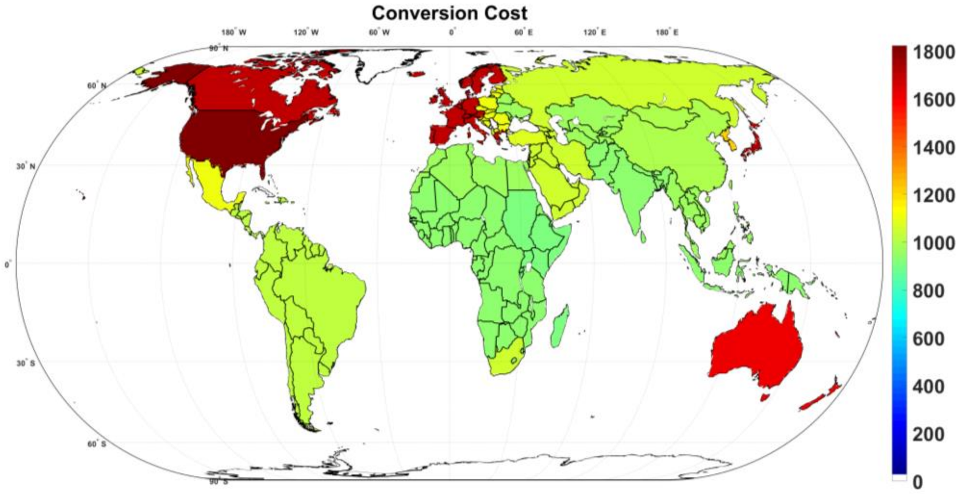
Conversion Cost
180° W
120° W
60° W
0°
60° E
120° E
180° E
90° N
60° N
30° N
0°
30° S
60° S
90° S
1800
1600
1400
1200
1000
800
600
400
200
0
€/ha

(b)

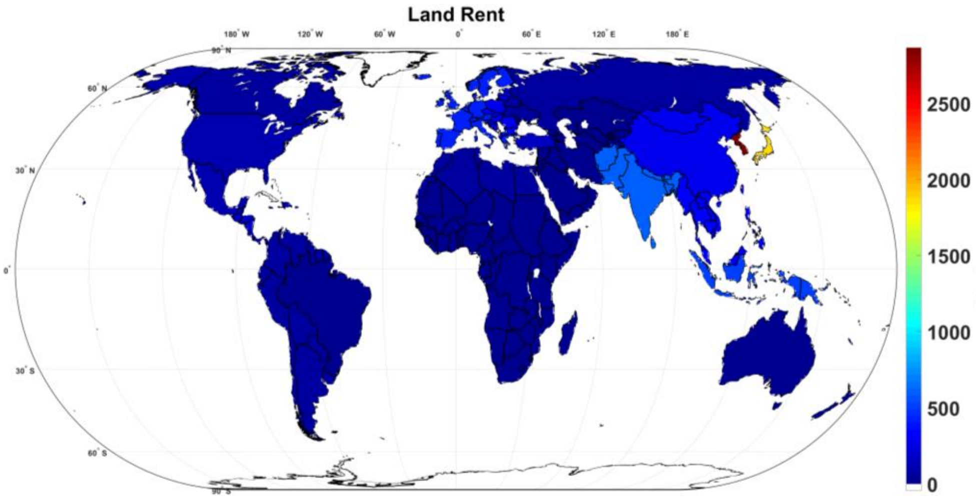
Land Rent
180° W
120° W
60° W
0°
60° E
120° E
180° E
90° N
60° N
30° N
0°
30° S
60° S
90° S
2500
2000
1500
1000
500
0
€/ha/year

(c)

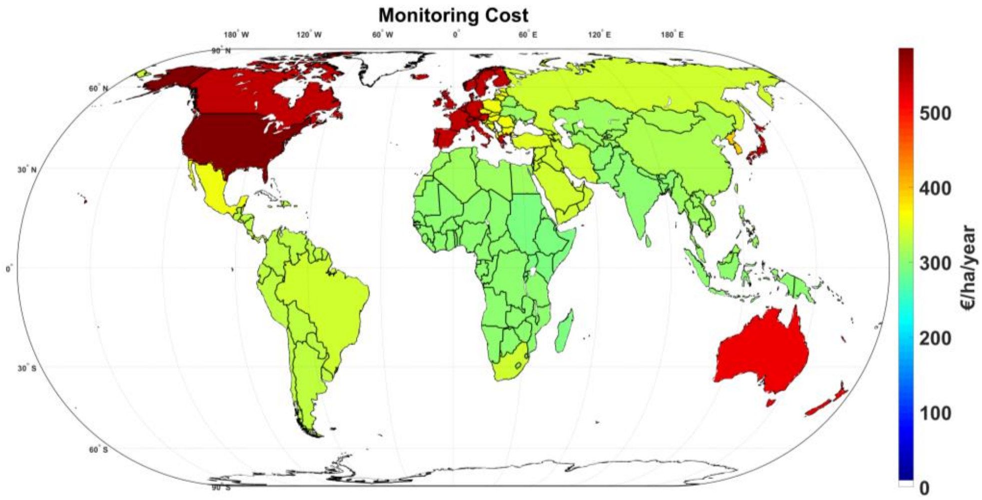
Monitoring Cost
180° W
120° W
60° W
0°
60° E
120° E
180° E
90° N
60° N
30° N
0°
30° S
60° S
90° S
500
400
300
200
100
0
€/ha/year

(d)

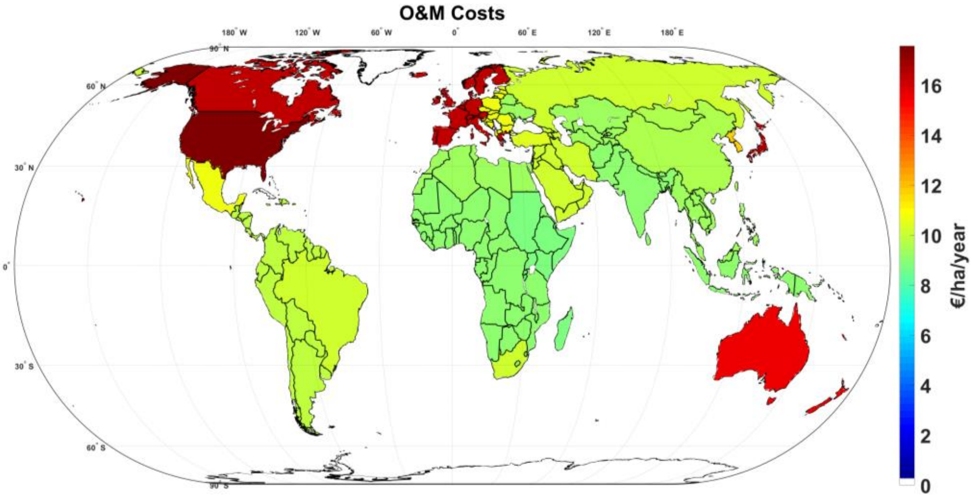

Figure S13. IMAGE model land costs obtained from Doelman et al.[10] and inflated to €2020, given per unit hectare: Conversion costs include site preparation, planting and assumed to be an initial cost (a); Land rent for agricultural land , maybe different for desert land (b); Monitoring costs for forests (c); operation and maintenance of infrastructure taken to be 3% of the conversion costs (d).

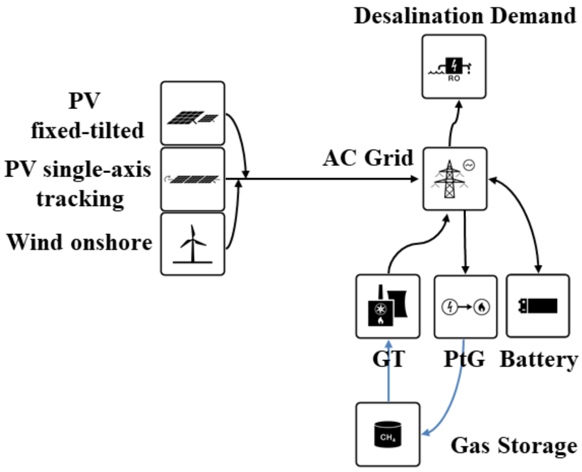

Figure S14. Version of LUT Energy System Transition Model[11–13] used to model the energy system for the SWRO desalination plants to provide water for the afforestation sites. The objective is to design a cost optimised energy system where the energy demand is met for every hour through different RE technologies. The technical and financial parameters of the energy system are provided in Manjong et al.[14], while the desalination system components are provided in Caldera and Breyer[9]. A complete version of the LUT Energy System Transition Model (LUT-ESTM) and the model functions that comprise the LUT-ESTM are presented in Bogdanov et al.[13] and Bogdanov et al.[11]

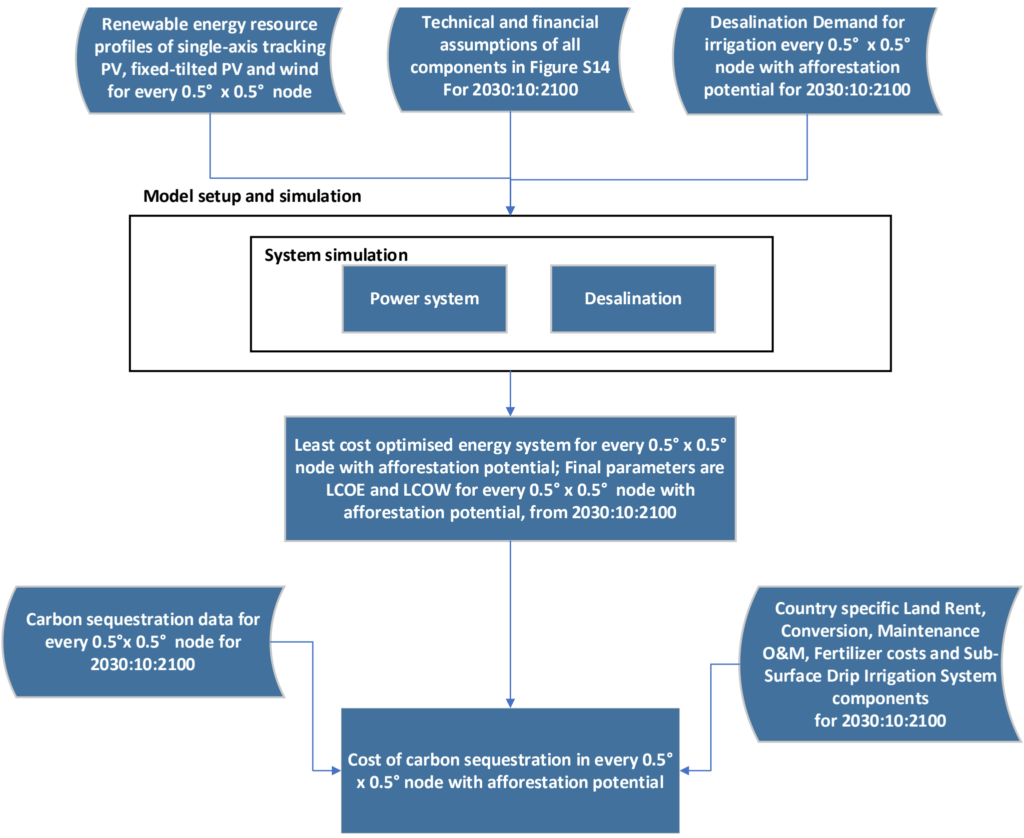

Figure S15. Flowchart of the processes involved with LUT-ESTM. In this research, LUT-ESTM is used to determine for every 0.5° x 0.5° node, the least cost energy system built on renewable resources in the area to meet the electricity demand of the desalination plants for the node in ten-year time steps for the period from 2030 to 2100. The capacities, generation and costs of the subsequent energy system for the period from 2030 to 2100 is used to obtain the levelised cost of electricity (LCOE) and the levelised cost of water (LCOW). Th*ese* data are used in conjunction with country specific land data and irrigation data to get the costs of carbon sequestration.

Table S2. Power density projection for ground mounted fixed-tilted PV, single-axis tracking PV, onshore wind power plant capacities installed in the specific years. Current and projected land area use of the solar PV technologies are obtained from Bolinger and Bolinger[15], projected for efficiency improvements based on Vartiainen et al. [16]. The wind power density numbers are from Bogdanov and Breyer[17]. Power densities are assumed to be the same for all technologies after 2050.

Years		**2030**	**2040**	**2050**	**2100**
PV fixed-tilted	MW/km^2	109.3	127.5	136.6	136.6
PV single-axis tracking	MW/km^2	74.1	87.4	93.6	93.6
Wind onshore	MW/km^2	8.4	8.4	8.4	8.4

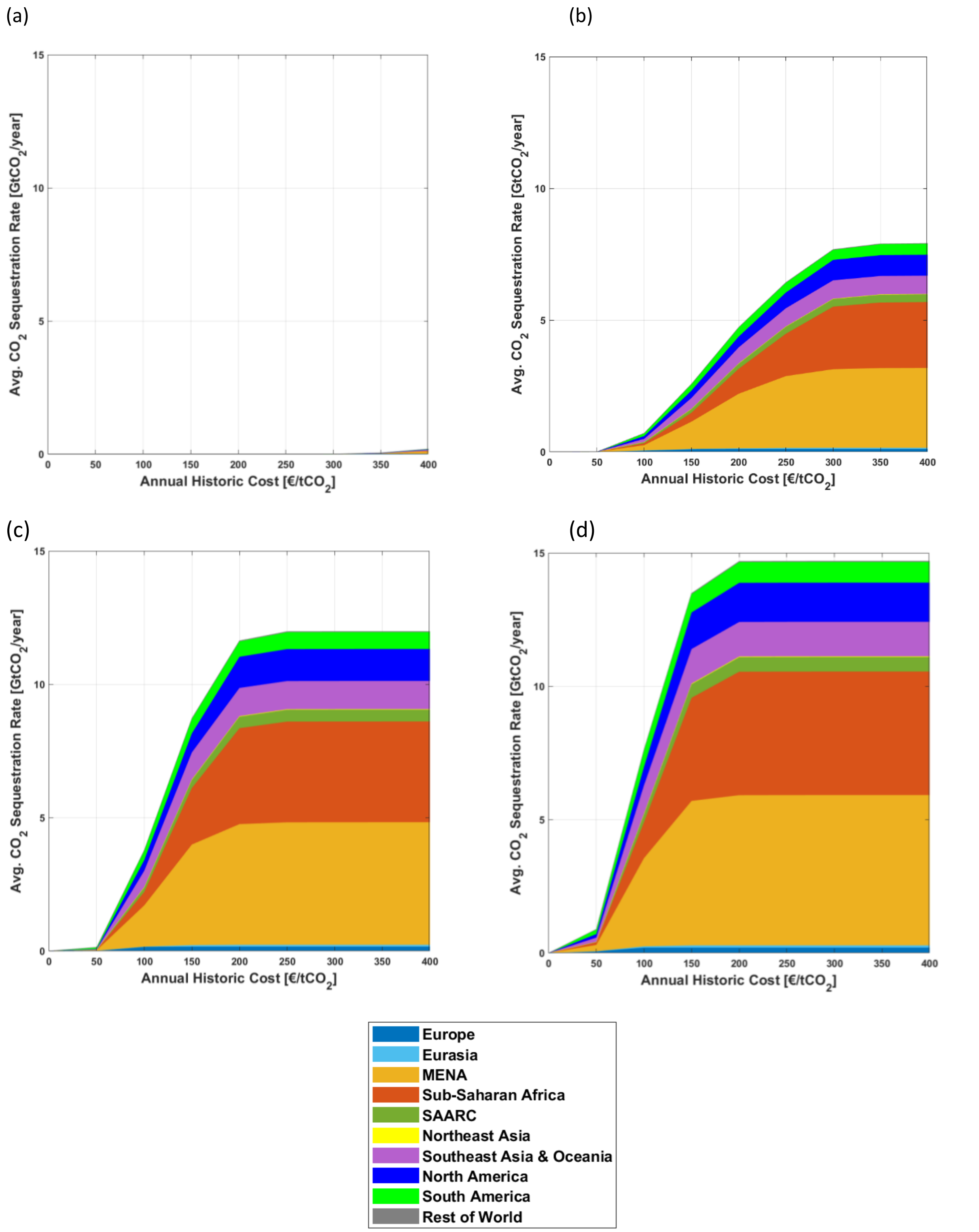

Figure S16. The average CO_2 sequestration rate per major region for different cost levels (€/tCO_2) for the years 2030 (a); 2050 (b); 2070 (c); 2100 (d). The legend represents the colours for the different regions.

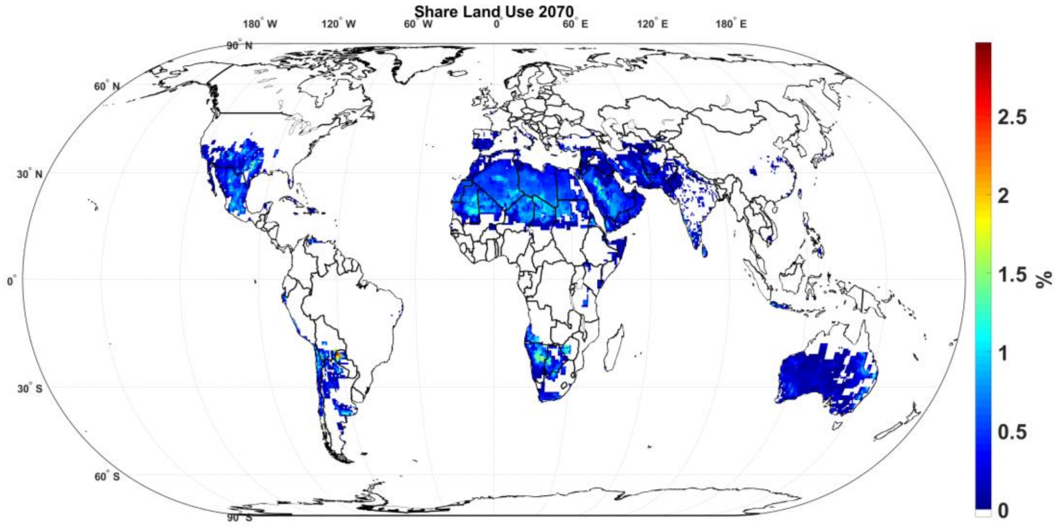

Figure S17. Share of land area of each 0.5° x 0.5° node with afforestation potential required for the fixed-tilted PV, single-axis tracking PV and onshore wind power plants in the year 2070. The land use is based on the numbers given in Table S2. On a global average, the total land area share for the renewable energy power plants is about 0.4%. Some nodes have relatively higher energy demand due to higher desalination demand and/or water pumping demands. Thus, these nodes have a land area usage higher than 1%. Supplementary Information 3 provides these numbers on a country average for the period from 2030 to 2100.

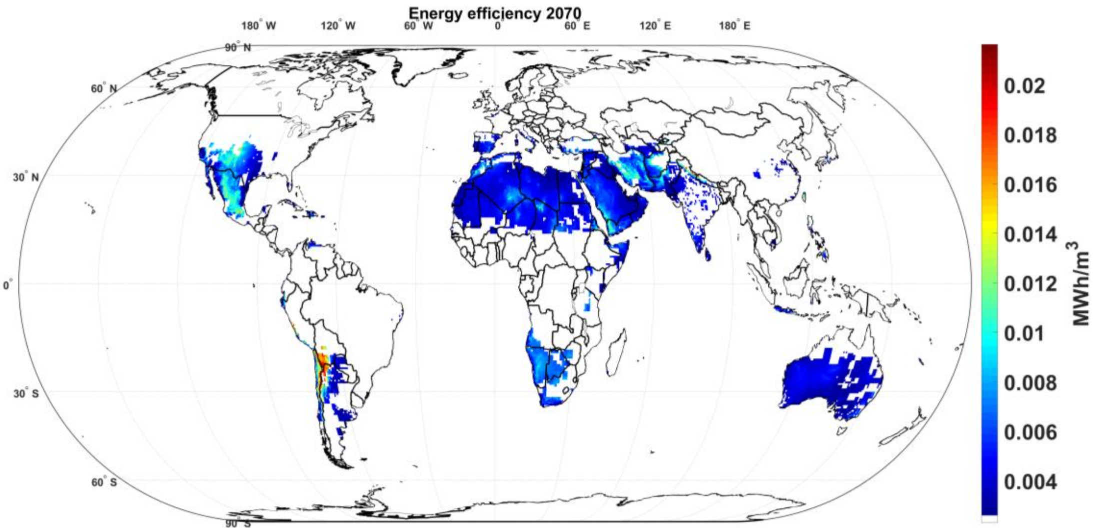

Figure S18. Total energy demand per m^3 of desalinated water produced for every 0.5° x 0.5° node with afforestation potential, for the year 2070. Supplementary Information 3 provides these numbers on a country average for the period from 2030 to 2100. The global average is about 0.005 MWh/m^3, but increases for regions in countries like Iran, USA, Mexico and Chile to between 0.01-0.02 MWh/m^3. The average energy demand to generate room temperature water for commercial atmospheric water generators (AWG) machines is about 0.98 MWh/m^3 [18–20]. This is a factor of 200 higher than that of the current research of 0.005 MWh/m^3. For places away from the coastline such as in Iran, Chile and USA the energy demand is a factor of 50-100 higher. The financial and technical parameters in current literature are based on small AWG machines that have a production capacity of 10.45 litres of water per day and a total investment cost of 2000 USD [18–20]. AWG machines are still in its infancy and therefore, from an energy and cost point of view do not compete with the more mature SWRO desalination plants. In the future with steep improvements in energy efficiency and reduction in cost, AWG may become a viable water source in regions that are further away from the coastline such as in Iran, USA and Chile.

References

1. Bastin, J. F. *et al.* The global tree restoration potential. *Science (80-.).* **364**, 76–79 (2019).
2. NASA Langley Research Center. Prediction Of Worldwide Energy Resources. (2018).
3. United States Department of Agriculture. Plant Hardiness Zone Map. (2012).
4. Center for Urban Forest Research. CUFR Tree Carbon Calculator. (2021).
5. Food and Agricultural Organisation of the United Nations. Chapter IV: Climatic Requirements of Date Palm. (2002).
6. FAO-UN Land and Water Division. FAO Map Catalog - Reference Evapotranspiration (Global - Mean Yearly - ~19km). (2004).
7. Pausata, F. S. R. *et al.* The Greening of the Sahara: Past Changes and Future Implications. *One Earth* **2**, 235–250 (2020).
8. Kemena, T. P., Matthes, K., Martin, T., Wahl, S. & Oschlies, A. Atmospheric feedbacks in North Africa from an irrigated, afforested Sahara. *Clim. Dyn.* **50**, 4561–4581 (2018).
9. Caldera, U. & Breyer, C. Strengthening the global water supply through a decarbonised global desalination sector and improved irrigation systems. *Energy* **200**, (2020).
10. Doelman, J. C. *et al.* Afforestation for climate change mitigation: Potentials, risks and trade-offs. *Glob. Chang. Biol.* **26**, 1576–1591 (2020).
11. Bogdanov, D. *et al.* Radical transformation pathway towards sustainable electricity via evolutionary steps. *Nat. Commun.* **10**, 1–16 (2019).
12. Bogdanov, D. *et al.* Low-cost renewable electricity as the key driver of the global energy transition towards sustainability. *Energy* **227**, (2021).
13. Bogdanov, D., Gulagi, A., Fasihi, M. & Breyer, C. Full energy sector transition towards 100% renewable energy supply: Integrating power, heat, transport and industry sectors including desalination. *Appl. Energy* **283**, (2021).
14. Manjong, N. B., Oyewo, A. S. & Breyer, C. Setting the Pace for a Sustainable Energy Transition in Central Africa: The Case of Cameroon. *IEEE Access* **9**, 145435–145458 (2021).
15. Bolinger, M. & Bolinger, G. Land Requirements for Utility-Scale PV: An Empirical Update on Power and Energy Density. *IEEE J. Photovoltaics* **12**, 589–594 (2022).
16. Vartiainen, E., Masson, G., Breyer, C., Moser, D. & Román Medina, E. Impact of weighted average cost of capital, capital expenditure, and other parameters on future utility-scale PV levelised cost of electricity. *Prog. Photovoltaics Res. Appl.* **28**, 439–453 (2020).
17. Bogdanov, D. & Breyer, C. North-East Asian Super Grid for 100% renewable energy

supply: Optimal mix of energy technologies for electricity, gas and heat supply options. *Energy Convers. Manag.* **112**, 176–190 (2016).

18. Shafeian, N., Ranjbar, A. A. & Gorji, T. B. Progress in atmospheric water generation systems: A review. *Renew. Sustain. Energy Rev.* **161**, 112325 (2022).

19. Asiabanpour, B., Ownby, N., Summers, M. & Moghimi, F. Atmospheric water generation and energy consumption: An empirical analysis. *2019 IEEE Texas Power and Energy Conference, TPEC 2019* 1–6 (2019) doi:10.1109/TPEC.2019.8662164.

20. Kandeal, A. W. *et al.* Research progress on recent technologies of water harvesting from atmospheric air: A detailed review. *Sustain. Energy Technol. Assessments* **52**, (2022).